

RESEARCH PAPER



The *Aspergillus fumigatus* farnesyltransferase β -subunit, RamA, mediates growth, virulence, and antifungal susceptibility

Tiffany S. Norton^a, Qusai Al Abdallah^b, Amy M. Hill^a, Rachel V. Lovingood^a, and Jarrod R. Fortwendel^b

^aDepartment of Microbiology and Immunology, University of South Alabama, Mobile, AL, USA; ^bDepartment of Clinical Pharmacy, University of Tennessee Health Science Center, Memphis, TN, USA

ABSTRACT

Post-translational prenylation mechanisms, including farnesylation and geranylgeranylation, mediate both subcellular localization and protein-protein interaction in eukaryotes. The prenyltransferase complex is an $\alpha\beta$ heterodimer in which the essential α -subunit is common to both the farnesyltransferase and the geranylgeranyltransferase type-I enzymes. The β -subunit is unique to each enzyme. Farnesyltransferase activity is an important mediator of protein localization and subsequent signaling for multiple proteins, including Ras GTPases. Here, we examined the importance of protein farnesylation in the opportunistic fungal pathogen *Aspergillus fumigatus* through generation of a mutant lacking the farnesyltransferase β -subunit, *ramA*. Although farnesyltransferase activity was found to be non-essential in *A. fumigatus*, diminished hyphal outgrowth, delayed polarization kinetics, decreased conidial viability, and irregular distribution of nuclei during polarized growth were noted upon *ramA* deletion ($\Delta ramA$). Although predicted to be a target of the farnesyltransferase enzyme complex, we found that localization of the major *A. fumigatus* Ras GTPase protein, RasA, was only partially regulated by farnesyltransferase activity. Furthermore, the farnesyltransferase-deficient mutant exhibited attenuated virulence in a murine model of invasive aspergillosis, characterized by decreased tissue invasion and development of large, swollen hyphae *in vivo*. However, loss of *ramA* also led to a Cyp51A/B-independent increase in resistance to triazole antifungal drugs. Our findings indicate that protein farnesylation underpins multiple cellular processes in *A. fumigatus*, likely due to the large body of proteins affected by *ramA* deletion.

ARTICLE HISTORY

Received 17 January 2017
Revised 2 May 2017
Accepted 4 May 2017

KEYWORDS



antifungal resistance; *Aspergillus*; farnesylation; farnesyltransferase; filamentous fungus; prenylation; Ras


Introduction

Protein farnesylation, one of 2 types of post-translational prenylation modification, plays an important role in the spatiotemporal regulation of many proteins. Farnesylation promotes membrane association of proteins by catalyzing the thioether linkage of a 15-carbon isoprenoid farnesyl moiety from farnesyl pyrophosphate to the CAAX-motif cysteine residue on the target protein. The C-terminal tetrapeptide “CAAX” motif (where C = cysteine, A = any aliphatic amino acid, and X = a variable amino acid) is the prenylation recognition sequence on target proteins. Farnesylation of CAAX motifs is an irreversible reaction and is catalyzed by the farnesyltransferase enzyme complex. The farnesyltransferase enzyme is a heterodimer composed of an α -subunit, shared with the structurally similar geranylgeranyltransferase type-I

complex, and a unique β -subunit.^{1,2} The identity of the “X” residue loosely determines prenyltransferase substrate specificity; X = methionine, serine, glutamine, cysteine, and alanine are classically associated with farnesylation, and X = leucine with geranylgeranylation.^{1,3-6}

Deletion of either farnesyltransferase subunit severely affects fungal growth in yeast-like fungi and, when examined in the human pathogenic yeast species, causes significant reductions in virulence. For example, deletion of the common prenyltransferase α -subunit is lethal in *Saccharomyces cerevisiae* and *Candida albicans*, likely due to the resulting complete lack of protein prenylation in these mutants.^{7,8} Additionally, deletion of the farnesyltransferase β -subunit has been reported in *S. cerevisiae* (*RAM1*), *Schizosaccharomyces pombe* (*cpp1*⁺),

CONTACT Jarrod R. Fortwendel  jfortwen@uthsc.edu  Clinical Pharmacy, University of Tennessee, 881 Madison Ave., Rm 343, Memphis, TN 38163, USA.

 Supplemental data for this article can be accessed on the [publisher's website](#).

© 2017 Tiffany S. Norton, Qusai Al Abdallah, Amy M. Hill, Rachel V. Lovingood, and Jarrod R. Fortwendel. Published with license by Taylor & Francis.

This is an Open Access article distributed under the terms of the Creative Commons Attribution-NonCommercial-NoDerivatives License (<http://creativecommons.org/licenses/by-nc-nd/4.0/>), which permits non-commercial re-use, distribution, and reproduction in any medium, provided the original work is properly cited, and is not altered, transformed, or built upon in any way.

and recently *Cryptococcus neoformans* (*RAM1*). Although not lethal in these yeast organisms, β -subunit deletion results in poor or no growth at lower temperatures (25–30°C) and a complete inability to support growth at 37°C, a factor critical to virulence.^{8–10} In contrast to the yeast-like fungi, the importance of farnesyltransferase activity has not been explored in filamentous fungi.

Aspergillus fumigatus is a ubiquitous filamentous fungal pathogen responsible for causing invasive aspergillosis (IA), a disease associated with a 40–90% mortality rate in the immunocompromised population.¹¹ The extraordinary ability of *A. fumigatus* to produce invasive disease derives in part from its proficiency in maintaining proper hyphal morphogenesis under host-induced environmental stress. In this study, we sought to determine the contribution of protein farnesylation to hyphal development and virulence of this important human pathogen. We report the first successful deletion of a farnesyltransferase β -subunit, named RamA here, in a mold fungus. Although loss of farnesyltransferase activity was not lethal in *A. fumigatus*, *ramA* deletion resulted in growth abnormalities including impaired hyphal branching, delayed conidial germination, reduced conidial viability, and aberrant distribution of nuclei in growing hyphae. As a marker for loss of farnesyltransferase activity, we show that *ramA* deletion displaces the predicted farnesylation target RasA from the plasma membrane. Additionally, loss of *ramA* was associated with attenuated virulence in a neutropenic murine model of invasive aspergillosis, yet reduced susceptibility to the antifungal drug voriconazole.

Results

Loss of protein farnesylation impairs *A. fumigatus* hyphal growth

We previously identified the gene encoding the *A. fumigatus* farnesyltransferase β -subunit via BLAST analysis of the *Aspergillus* genome database (aspergillusgenome.org) using the *S. cerevisiae* *RAM1* sequence as a query.¹² The *A. fumigatus* genome contains a single *RAM1*-homologous gene (Afu4g10330) that comprises 7 exons and encodes a predicted protein product of 519 amino acids with a molecular weight of 56.6 kDa. BLASTP alignment of predicted Ram1-homolog proteins revealed sequence identities of 38% and 69% between the *A. fumigatus* sequence and the *S. cerevisiae* and *A. nidulans* sequences, respectively. Because it represents the sole *RAM1* homolog in *A. fumigatus*, we have named this gene *ramA*.

To explore roles for farnesyltransferase activity in *A. fumigatus* growth and virulence, a *ramA* deletion strain

was generated. The entire *ramA* coding region was replaced with a deletion cassette containing the hygromycin resistance marker, using established *Aspergillus* transformation protocols. To confirm that all observed phenotypes in the *ramA* deletion strain ($\Delta ramA$) were solely a result of *ramA* targeting, a complemented strain was generated by ectopic re-integration of the *ramA* coding region. Initial examination revealed that the $\Delta ramA$ mutant exhibited a deficiency in radial growth rate on GMM agar (Fig. 1A). Significant differences in colony diameter were observed after 48, 72 and 96 hours of growth at 37°C, with the $\Delta ramA$ mutant colony reaching only 51.2% of the diameter of the wild type (WT) strain at 96 hours (Fig. 1B). Reduced growth of the $\Delta ramA$ strain was independent of media composition (Fig. S1A). However, growth reduction caused by loss of *ramA* was not associated with aberrancies in conidial development. No significant differences were noted in the total number of conidia produced for each strain, regardless of media composition (Fig. 1C and Fig. S1B). Additionally, despite the reduced radial outgrowth, the $\Delta ramA$ mutant displayed largely normal hyphal morphogenesis (Fig. 1D).

RamA controls the timing of polarity establishment and nuclear population of conidia

Polarity establishment, defined at the earliest time points by anisotropic conidial morphology, was delayed by approximately 2 hours in the $\Delta ramA$ mutant (Fig. 2A). Furthermore, the rate of polarity establishment was slowed in the $\Delta ramA$ mutant when compared with the WT. Only 45.6% ($\pm 9.1\%$) of $\Delta ramA$ conidia had formed germ tubes at 12 hours post-inoculation, by which time 100% of the conidia from the WT and complemented strains had an established polarized growth axis. At 24 hours post-inoculation, only 51.7% ($\pm 6.5\%$) of the $\Delta ramA$ conidia had formed a germ tube (Fig. 2A). The conidia remaining in the $\Delta ramA$ culture after 24 hours appeared dormant, with no swelling evident, indicating decreased conidial viability (data not shown).

To test whether the observed conidial viability deficit in the $\Delta ramA$ mutant arose from *a priori* anucleate conidia, we first generated conidiophores on GMM agar using a slide culture technique.¹³ The cell wall and nuclear DNA in newly-formed conidia from conidiophores generated by this technique were visualized with calcofluor white (CFW) and propidium iodide (PI) staining, respectively. Examination of the stained conidia from each strain revealed that only 57% ($\pm 4.0\%$) of $\Delta ramA$ conidia were positive for PI staining (Fig. 2B–C). This measurement corresponded to the 51.7% ($\pm 6.5\%$) of $\Delta ramA$ conidia that were capable of germination (Fig. 2A). In contrast, 92% ($\pm 1.5\%$) of WT conidia were

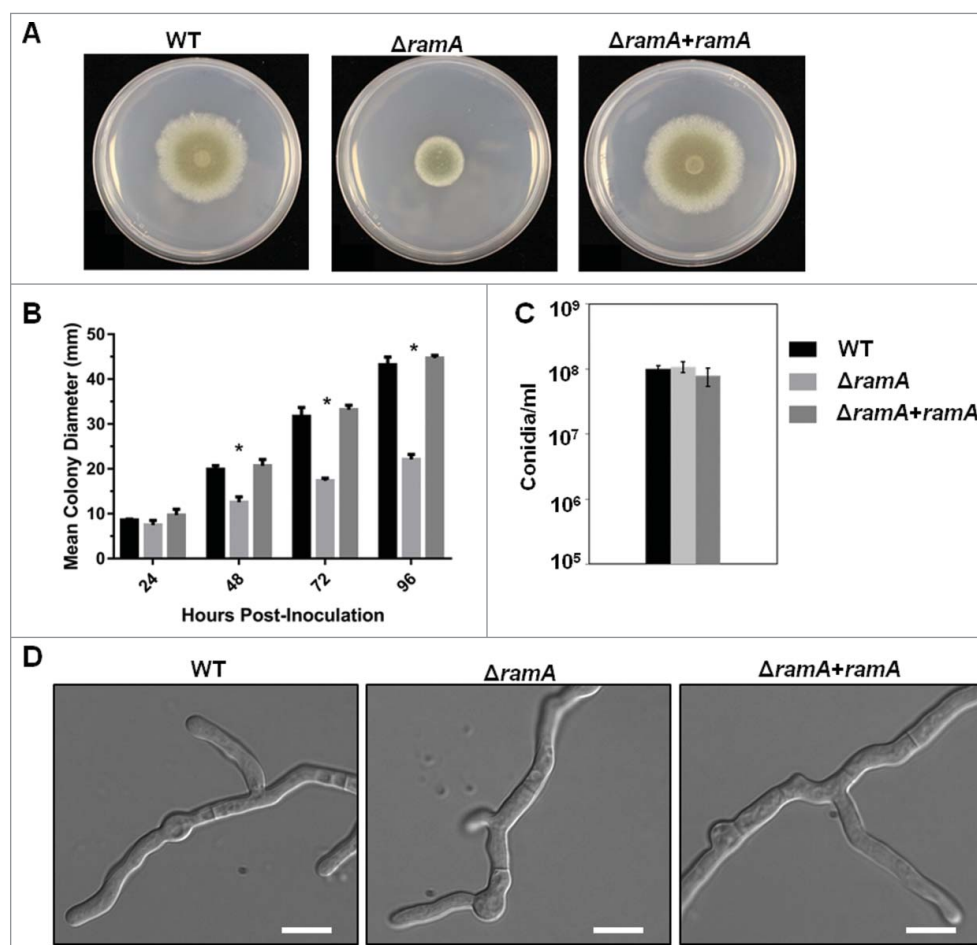


Figure 1. *A. fumigatus* RamA regulates hyphal growth. (A) Colony morphology of the *ramA* isogenic set. GMM agar plates were inoculated with a 10 μ l drop containing 1×10^4 conidia and incubated at 37°C for 96 hours. (B) Colony diameters of the *ramA* isogenic set measured at 24-hour intervals over the 96-hour incubation period. Measurements and error bars represent the mean and standard deviation (SD) of 3 independent experiments. Colony diameters between strains at each 24-hour interval were compared using 2-way ANOVA with Tukey's test for multiple comparisons (GraphPad Prism v7). Asterisks above the $\Delta ramA$ strain measurement bars indicate a statistically significant difference (adjusted *p* value < 0.001) between the $\Delta ramA$ strain and both the WT and reconstituted strains at the indicated time point. (C) Comparison of conidia generated by the isogenic set during culture on GMM. A 1 ml suspension of freshly harvested conidia at a concentration of 1×10^6 conidia/ml was spread evenly onto GMM agar and cultured for 3 d at 37°C. Conidia were harvested and enumerated on a hemocytometer. Experiments were performed in triplicate. No significant differences between strains were noted (*p* value > 0.05). (D) Hyphal morphology of the *ramA* isogenic set. Two thousand conidia from each strain were inoculated into GMM broth and incubated over sterile coverslips for 16 hours at 37°C. Scale bars represent 10 μ m.

PI positive (Fig. 2C). These results are in line with the hypothesis that *ramA* deletion leads to increased generation of anucleate conidia and thus a conidial viability deficit. Additionally, the significant delay in the initiation of polarity noted among viable $\Delta ramA$ conidia suggests that protein farnesylation is required for timely polarity establishment in *A. fumigatus*.

Deletion of *ramA* results in increased variability of nuclear number in hyphal compartments

The results presented above suggested that *ramA* deletion results in irregular segregation of nuclei into

nascent conidia. To test whether the $\Delta ramA$ mutant exhibited additional aberrancies in nuclear distribution at other developmental stages, we next examined portioning of nuclei in growing hyphae. Conidia of the *ramA* isogenic set were incubated to enrich for 3 distinct developmental stages,¹⁴ and cell walls and nuclear DNA visualized by CFW/PI staining. The 3 developmental stages included the following: 1) swollen conidia (SC), representing the initial break from dormancy; 2) early germlings (EG), representing unicellular germinated conidia with short germ tubes which have undergone mitosis but not yet undergone septation; and 3) growing hyphae (GH), representing

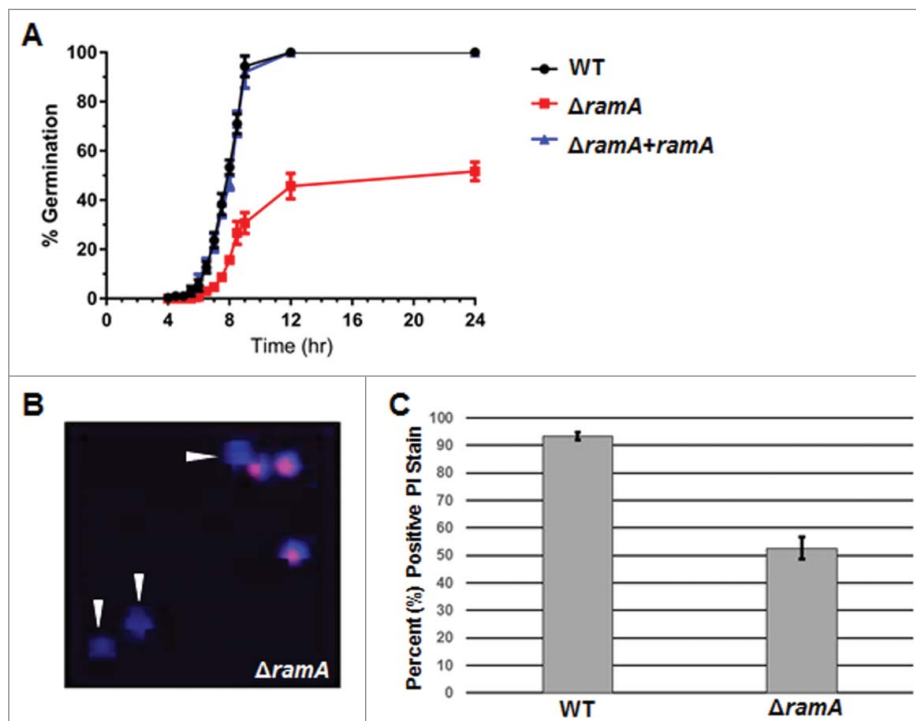


Figure 2. Deletion of *ramA* delays polarity establishment and viability. (A) Polarity establishment rates of the *ramA* isogenic set. Conidia (1×10^6) of each strain were inoculated on sterile coverslips submerged in GMM broth and incubated at 37°C. At the designated time points, coverslips were mounted for bright field microscopy, and one hundred conidia were examined. The percent of polarized germlings was scored as the number of conidia which had produced a visible germ tube at that time point. Measurements and error bars represent the mean and standard error of the mean (SEM) of 3 independent experiments. (B) Conidia of the $\Delta ramA$ strain were stained with propidium iodide (PI, red) to detect nuclear material and with calcofluor white (CFW, blue) to detect chitin in cell walls. Arrowheads denote CFW-stained conidia in which no nuclear material is detected. (C) One hundred PI-stained conidia of the wild type (WT) and $\Delta ramA$ strains were examined by fluorescence microscopy, and percent positive PI staining was scored. Results are the average of 3 independent experiments (\pm SD).

a later stage of hyphal elongation after septal formation and multiple mitotic divisions.

SC and EG exhibited no significant difference in the number of nuclei per cell between strains of the isogenic set. The SC of each strain contained one to 2 nuclei each, whereas EGs of each strain contained an average of 2 to 4 nuclei (Fig. 3B). However, the positioning of nuclei within $\Delta ramA$ EGs differed from the WT and complement strain. Nuclei in the $\Delta ramA$ EGs were clustered near the site of the emerging germ tube, in contrast to the WT and complement strains which exhibited uniformly distributed nuclei (Fig. 3A, top). Significant aberrancies in both measures of nuclear distribution were especially apparent in the later stages of GH of $\Delta ramA$. Although the mean nuclear number of interseptal compartments was not significantly different between the strains, nuclei appeared irregularly spaced within the GH of the $\Delta ramA$ mutant (Fig. 3A–B). Based on these observations, we performed a quantitative analysis to measure $\Delta ramA$ deviation from WT in terms of variability of nuclear number. Quantitative comparison of the mean standard deviations produced by enumerating nuclei within interseptal compartments of GH for each strain confirmed that

variability between strains was significantly different at this stage, with $\Delta ramA$ displaying increased variability (Fig. 3C). These results suggest that nuclear positioning in GH is impacted by protein farnesylation.

Farnesylation mediates *RasA* localization and activation

Complete abrogation of *RasA* prenylation by mutating the CAAX-motif cysteine to a serine mislocalizes *RasA* to the cytoplasm.¹⁵ These earlier results indicated that either post-translational farnesylation or geranylgeranylation is required for *RasA* association with cellular membranes. Therefore, we assessed the effect of farnesyltransferase deletion on *RasA* localization by expressing a GFP-*RasA* fusion protein in the $\Delta ramA$ mutant. GFP fluorescence in the $\Delta ramA$ +GFP-*RasA* strain was spread diffusely throughout the cytosol (Fig. 4A), with significant membrane-localized GFP signal retained only at septal membranes. This distribution was in stark contrast to the defined GFP signal along the plasma membrane seen in a strain with intact farnesylation activity (Fig. 4A). Quantitative analysis of localization confirmed a weak retention of

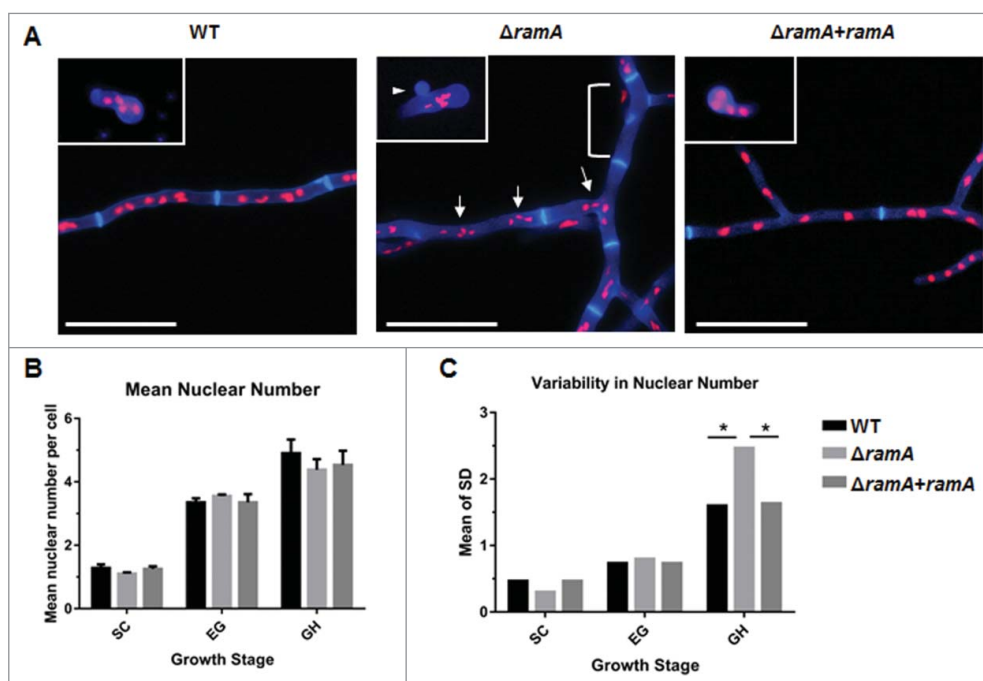


Figure 3. RamA is required for normal nuclear distribution in growing hyphae. (A) Nuclear positioning within germlings and hyphal compartments of the *ramA* isogenic set. 1×10^5 conidia of each strain were inoculated onto sterile coverslips submerged in GMM broth and incubated at 37°C for various time points to enrich for selected growth stages. Incubation times were based on the germination assay results in Fig. 2 [Swollen conidia (SC): WT, $\Delta ramA+ramA$ = 5.5 hours; $\Delta ramA$ = 6 hours. Early germling (EG): WT, $\Delta ramA+ramA$ = 6.5 hours; $\Delta ramA$ = 7.5 hours. Growing hyphae (GH): all strains = 16 hours.]. Coverslips were fixed and stained with CFW to visualize the cell wall and PI to visualize nuclei. Representative micrographs of each strain are shown. Inset images are from the EG stage, whereas the main panel displays GH stage for each strain. Note the anuclear conidium, denoted by the white arrowhead, in the $\Delta ramA$ EG inset micrograph. Scale bars represent 20 μ m. (B) Mean nuclear number per cell of the *ramA* isogenic set. The number of nuclei within 20 conidia, germlings, or subapical interseptal compartments was enumerated. Nuclei were identified as discrete spots of PI staining within the cell boundaries outlined with CFW. Measurements represent the mean of 3 independent experiments (\pm SD). The mean nuclear number was not statistically different between any strains at any tested growth stage. (C) Variability of nuclear number in cells of the *ramA* isogenic set. The SD was calculated for each combination of strain and growth stage for each of the 3 experimental replicates in (B). Variability was defined as the overall mean of the SDs of the 3 experimental replicates for each combination of strain and growth stage. Statistics were computed by 2-way ANOVA with Tukey's test for multiple comparisons (*, $p < 0.05$).

RasA at the plasma membrane and clear accumulation at the septa in the absence of farnesyltransferase activity (Fig. 4B). To inspect the effect of loss of RasA farnesylation on its activation, we performed a Ras activation assay on the *ramA* isogenic set, isolating GTP-bound RasA with a Ras binding domain (RBD) polypeptide that binds RasA in a GTP-dependent manner. Immunoblotting revealed that although total RasA was decreased in the $\Delta ramA$ mutant as compared with the WT and reconstituted strains, the levels of GTP-bound RasA were increased (Fig. 4C). Densitometric analysis indicated that normalized levels of GTP-bound RasA in the $\Delta ramA$ mutant were almost double those of the wild type (Fig. 4D). These results demonstrate that lack of farnesylation does not negatively impact RasA activation in *A. fumigatus*.

A. fumigatus $\Delta ramA$ exhibits attenuated virulence

To test the importance of farnesyltransferase activity to virulence in *A. fumigatus*, we used a murine model

of invasive aspergillosis, as described previously.¹⁶ Mice were immunosuppressed with a regimen including cyclophosphamide and triamcinolone acetonide (Fig. 5A). Mice ($n = 14$ per treatment group) were inoculated with freshly harvested conidia of the *ramA* isogenic set, as well as a double concentration of $\Delta ramA$ conidia ($2x\Delta ramA$) to account for the observed viability deficit. Mortality was monitored for 14 d post-inoculation. Mice infected with the $\Delta ramA$ conidia exhibited decreased and delayed mortality compared with those infected with WT or reconstituted strains (Fig. 5A). Seventy-one percent of mice receiving $\Delta ramA$ conidia and 85% of mice receiving $2x\Delta ramA$ conidia survived until the termination of the study, compared with 21% percent of mice receiving WT conidia and 7% of mice receiving conidia of the reconstituted strain. The onset of death in mice inoculated with both concentrations of $\Delta ramA$ conidia was likewise delayed; notably, the sole death in mice infected with $2x\Delta ramA$ conidia occurred only

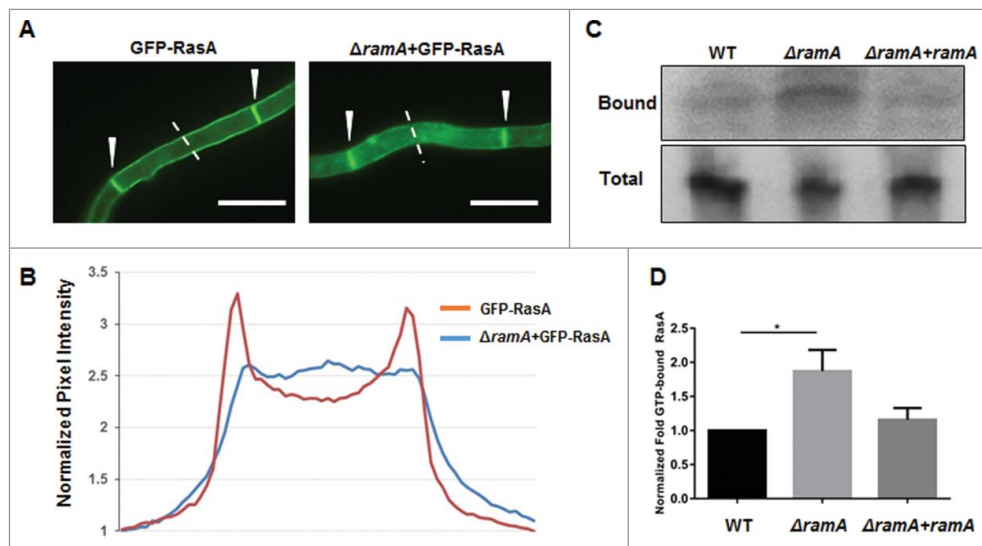


Figure 4. Loss of farnesyltransferase activity affects RasA localization to the plasma membrane. (A) Localization of RasA in the presence and absence of RamA-mediated farnesylation. A GFP-RasA fusion protein is localized to the plasma membrane and septa in the presence of RamA (GFP-RasA). RasA is partially mislocalized to the cytosol in the absence of farnesylation ($\Delta ramA$ +GFP-RasA). Note the strong presence of GFP signal at the septa in both the GFP-RasA and $\Delta ramA$ +GFP-RasA strains, indicated by white arrowheads. Scale bar represents 10 μm . (B) Quantitation of pixel intensity as representative quantitation of GFP-RasA localization. Pixel intensity was quantitated spanning hyphal cross-sections using the Nikon Advanced Research software package. Six independent measurements of background fluorescence in a single field (areas with no hyphal growth) were averaged for each strain and used to normalize the pixel intensity values. The graph is a representative quantitation of a single field and depicts the normalized intensities across the 8 μm dotted line pictured in panel (A). (C) Representative immunoblot of GTP-associated (i.e., activated) RasA (Bound) and total RasA (Total) in strains of the *ramA* isogenic set. (D) Densitometric analysis of immunoblots indicates that RasA activation is increased almost twofold in the $\Delta ramA$ mutant with respect to the wild type (WT) and complement ($\Delta ramA$ +*ramA*) strains. Measurements and error bars represent the mean of 3 independent experiments (\pm SD). Statistics were computed by one-way ANOVA with Dunnett's test for multiple comparisons (*, $p < 0.05$).

at Day 14 post-inoculation. Thus, the $\Delta ramA$ strain was significantly less virulent than the wild type.

To determine relative fungal burdens in the lungs of mice infected with WT and both concentrations of $\Delta ramA$ conidia versus uninfected (vehicle) control mice, we used a previously published qPCR assay.¹⁷ Comparisons did not reach statistical significance because of intra-group variability, but a trend was apparent (Fig. 5B). Fungal burden trended lower in mice infected with either concentration of $\Delta ramA$ conidia than with WT conidia, correlating with reduced growth *in vivo*. Histopathologic examination of lung sections confirmed that hyphal growth was greatly diminished in mice inoculated with either concentration of $\Delta ramA$ conidia compared with the WT (Fig. 5C, upper panels). H&E staining indicated that an inflammatory infiltrate accompanied the fungal lesions in mice infected with all strains (Fig. 5C, lower panels). Tissue from control mice contained neither lesions nor architectural changes indicating inflammation. Interestingly, lesions in mice inoculated with $\Delta ramA$ conidia featured dysmorphic hyphae with swollen, blebbed structures staining positively with GMS (Fig. 6). These morphological aberrancies were not observed when the $\Delta ramA$ mutant was

cultured *in vitro*, and were also not produced by the WT strain *in vivo* (Fig. 6), suggesting that the lung microenvironment or other host-related factors accentuate the growth deficiencies inherent in the $\Delta ramA$ mutant.

Farnesyltransferase activity is required to maintain hyphal morphology in response to nikkomycin Z

To try to recapitulate the invasive growth abnormalities of $\Delta ramA$, the isogenic set was cultured under various *in vitro* conditions chosen to mimic known *in vivo* stress. No significant differences in germination rate, growth rate, or morphology were noted in a variety of stress conditions, including dithiothreitol or brefeldin A to induce endoplasmic reticulum stress,¹⁸ iron-free media chelated with bathophenanthrolinedisulfonic acid to mimic an iron depleted environment,¹⁹ cobalt chloride to mimic a hypoxic microenvironment,²⁰ and hydrogen peroxide to induce oxidative stress. However, when cultured with nikkomycin Z, a specific inhibitor of chitin synthase activity, growth of the $\Delta ramA$ mutant was significantly inhibited by concentrations as low as 0.1 $\mu\text{g/ml}$ and displayed an MIC₅₀ of 1.6 $\mu\text{g/ml}$ (Fig. 7A). Complete inhibition of growth was achieved at 50 $\mu\text{g/ml}$ for the

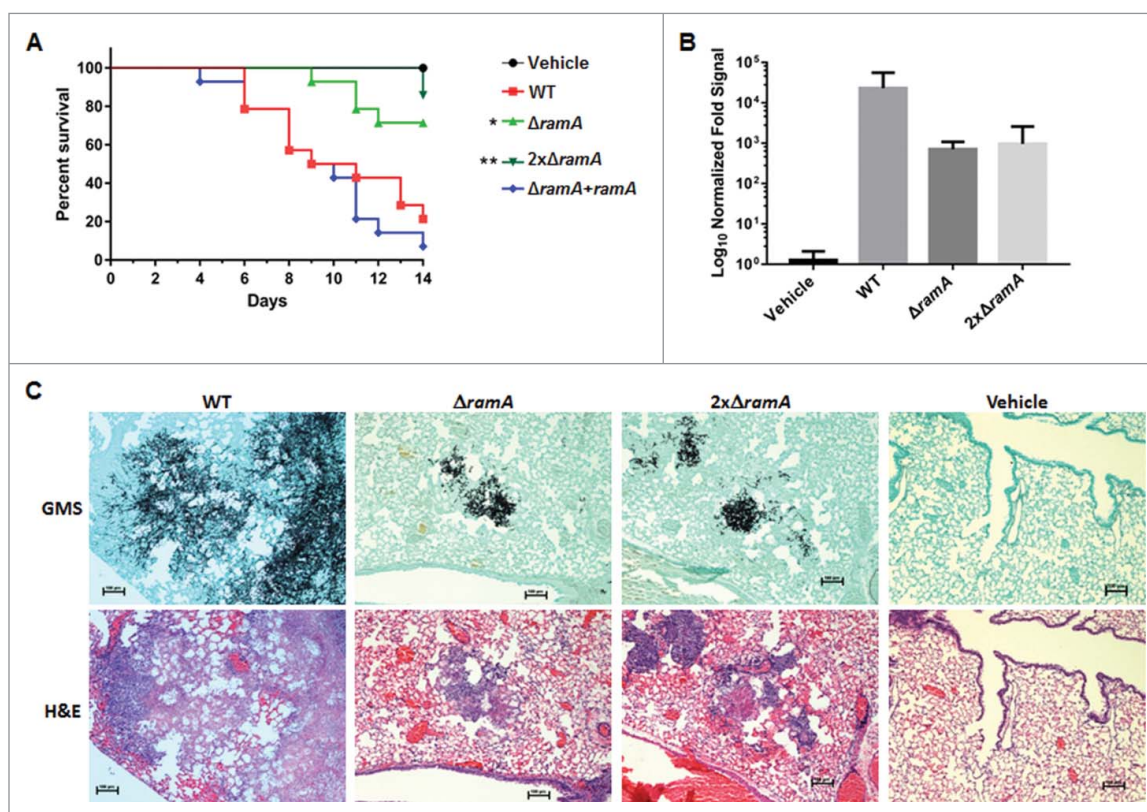


Figure 5. The $\Delta ramA$ mutant exhibits attenuated virulence in a neutropenic murine model of invasive aspergillosis. (A) Survival curve for neutropenic invasive aspergillosis model. Statistics were computed by Kruskal-Wallis analysis with Dunn's test for multiple comparisons. Asterisks indicate a statistically significant difference in survival ($p_{\Delta ramA} = 0.035$; $p_{2x\Delta ramA} = 0.003$) between WT and $\Delta ramA$ -related strains. (B) Quantitative PCR (qPCR) analysis of fungal burden in murine lungs harvested on Day 3 post-inoculation. Measurements represent the overall mean fold qPCR signal ($2^{-\Delta CT}$) of 3 technical replicates (\pm SD) from each of 3 mice, normalized to the mean signal from 3 uninfected control (vehicle) mice. Statistics were computed by one-way ANOVA with Dunnett's test for multiple comparisons. (C) Serial sections from murine lungs stained with Gomori methenamine silver (GMS) stain (upper panels) and hematoxylin and eosin (H&E) stain (lower panels). Note the reduced hyphal outgrowth in GMS-stained lesions from lungs of mice inoculated with $\Delta ramA$ strains. Scale bars represent 100 μ m.

$\Delta ramA$ mutant, whereas overall growth of the wild type was unimpaired (Fig. 7A). When examined microscopically, the $\Delta ramA$ was found to develop swollen hyphal segments, reminiscent of the *in vivo* growth phenotype, at concentrations that did not affect morphology of the wild type (Fig. 7B). No changes in sensitivity to caspofungin, a specific inhibitor of glucan synthesis, were noted using similar experimental studies. These data suggested that the cell wall defect of the $\Delta ramA$ mutant was specific to chitin biosynthesis.

The *A. fumigatus* $\Delta ramA$ mutant exhibits altered sensitivity to antifungals

To assess the effect of *ramA* deletion on the response to antifungals, we measured the minimum inhibitory concentration (MIC) to the ergosterol targeting compound, amphotericin B, the triazole-based ergosterol biosynthesis inhibitors, voriconazole and itraconazole, and the selective inhibitor of glucan synthesis,

caspofungin. MICs were determined by E-test assay on multiple media to ensure resulting phenotypes were independent of growth conditions. The MICs for voriconazole and itraconazole were consistently higher for the $\Delta ramA$ mutant on all media tested, when compared with the WT strain (Fig. 8 and Fig. 9A). For Amphotericin B, the opposite trend was noted. The $\Delta ramA$ mutant displayed a small but consistent decrease in Amphotericin B MIC (Fig. 8). As noted previously, no significant change in the MIC for caspofungin treatment was found by E-test assay (Fig. 8). Examination of susceptibility profiles by broth microdilution, using Clinical and Laboratory Standards Institute (CLSI) methodology,²¹ further confirmed the resistance associated with *ramA* deletion (Table S2). To see if triazole resistance was specific to loss of *ramA*, and not associated with other slow-growth mutants, we also examined sensitivity of a *rasA* deletion mutant ($\Delta rasA$) to voriconazole. Regardless of the media used, no changes in the

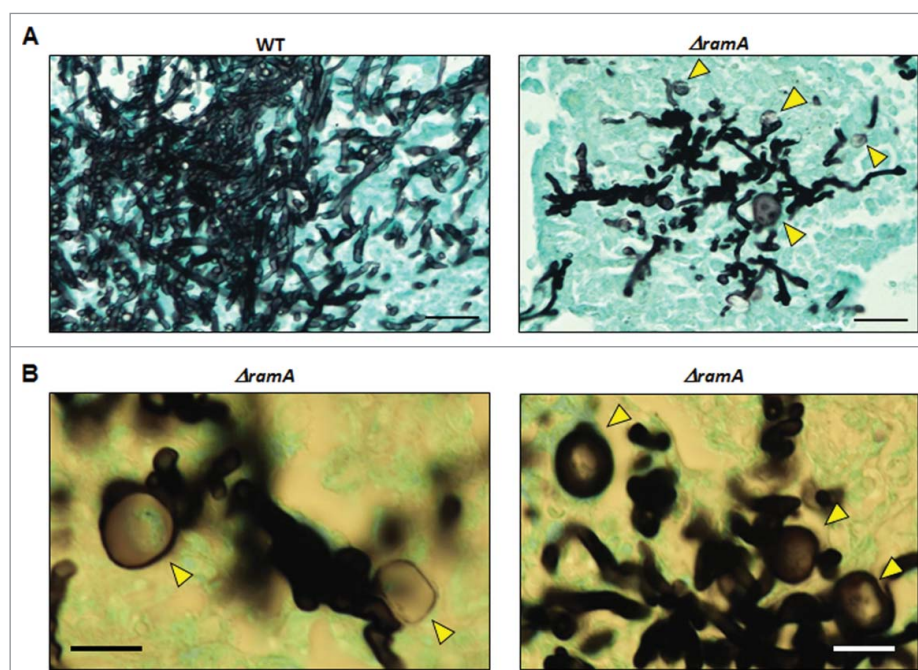


Figure 6. The $\Delta ramA$ mutant develops polarity defects *in vivo*. (A) Lesions formed by $\Delta ramA$ exhibit dysmorphic hyphal morphology and blebbed structures (yellow arrows) *in vivo*, indicating a loss of hyphal polarity. Scale bars represent 25 μm . (B) Higher magnification micrographs of *in vivo* hyphal morphology of the $\Delta ramA$ mutant. Yellow arrows denote swollen hyphal structures. Scale bars represent 12.5 μm .

susceptibility profile were induced by *rasA* deletion when analyzed by E-test or broth microdilution (Fig. S2 and Table S2). These data suggested that deletion of *ramA* specifically altered susceptibility to the antifungal compounds targeting ergosterol and its

biosynthesis. In addition, this phenotype is not likely to be mediated via RasA signaling.

A common mechanism for increased triazole resistance in *A. fumigatus*, and other pathogenic fungi, is the increased expression of the target genes required for

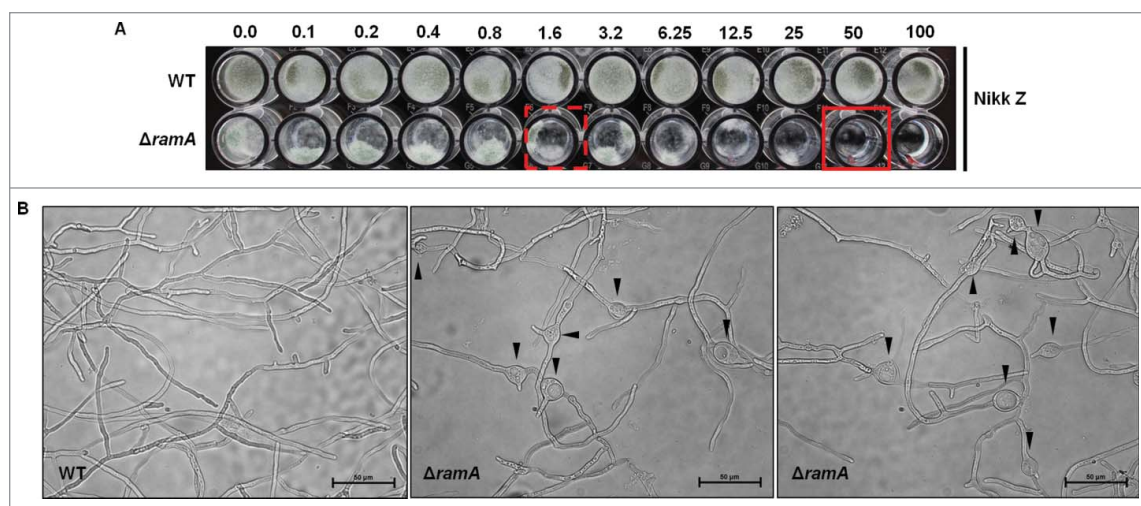


Figure 7. Farnesyltransferase activity is required to support hyphal morphogenesis in response to Nikkomycin Z. (A) Broth microdilution MIC analysis of the wild type (WT) and the $\Delta ramA$ mutant. Ten thousand conidia from the wild type and 20 thousand conidia from the $\Delta ramA$ mutant were inoculated into GMM liquid media with ascending doses of the specific chitin synthesis inhibitor, nikkomycin Z, and incubated for 48 hours at 37°C. 50% growth inhibition (MIC50) was noted for the $\Delta ramA$ mutant at 1.6 $\mu\text{g/ml}$ nikkomycin Z (dashed, red square) and complete growth inhibition at 50 $\mu\text{g/ml}$ (solid, red square). Nikkomycin Z MIC of the wt was not achieved (> 100 $\mu\text{g/ml}$). (B) Microscopic examination of hyphae from the wild type (wt, left panel) and the $\Delta ramA$ mutant (middle and right panels) grown for 24 hrs in GMM liquid media at 37°C in the presence of 1 $\mu\text{g/ml}$ nikkomycin Z. Black arrowheads denote swollen hyphal segments in the $\Delta ramA$ strain.

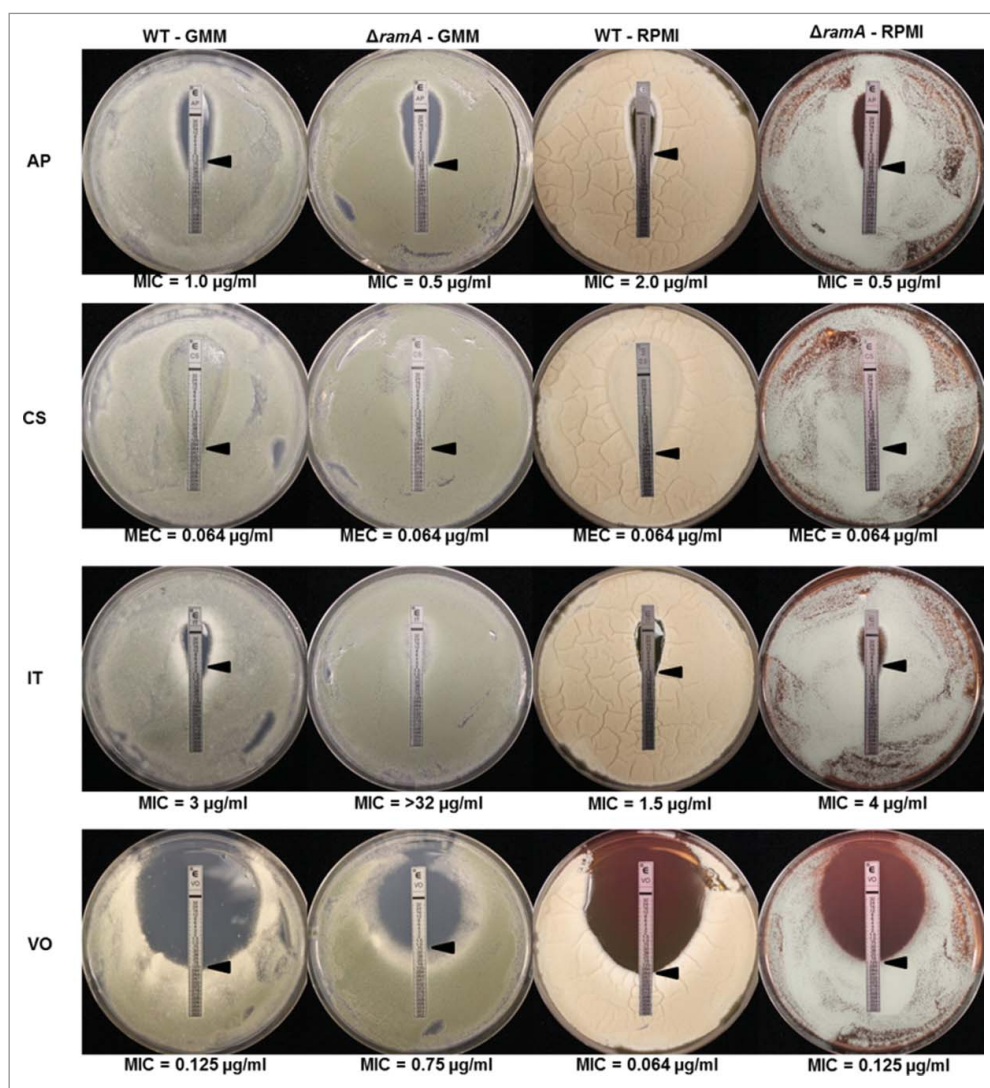


Figure 8. The $\Delta ramA$ mutant exhibits altered susceptibility profiles to antifungal drugs. The E-test method was used to delineate minimum inhibitory concentrations (MICs) for the wild type (WT) and $ramA$ deletion mutant ($\Delta ramA$) on GMM and RPMI agar. Antifungals tested were Amphotericin B (AP), Caspofungin (CS), Itraconazole (IT) and Voriconazole (VO). A small but consistent increase in susceptibility was noted for the $\Delta ramA$ mutant in the presence of AP. In contrast, moderate and consistent increases in MIC values were noted for the $\Delta ramA$ mutant in the presence of the triazoles, IT and VO. No changes in susceptibility were noted for the cell wall targeting compound, CS.

ergosterol biosynthesis.²² We therefore sought to determine whether increased *cyp51A* or *cyp51B* expression could be correlated with the increased triazole resistance of $\Delta ramA$. To obtain sufficient hyphal mass for extraction of high-quality RNA to perform expression analyses, the WT and $\Delta ramA$ strains were cultured in GMM+YE liquid media and exposed to a sub-MIC concentration of voriconazole before extraction. Voriconazole was chosen for our analyses as this is a frontline therapy for invasive aspergillosis. qRT-PCR assays were then performed to compare *cyp51A* and *cyp51B* transcript levels in the WT and $\Delta ramA$ mutant, based on a previously published protocol.²³ Statistical analyses revealed no significant differences in the transcript abundance of *cyp51A* or *cyp51B* in the $\Delta ramA$ mutant when compared with the

WT strain, regardless of the presence or absence of voriconazole (Fig. 9B). These findings suggested a non-*cyp51*-dependent mechanism leading to decreased triazole susceptibility when farnesyltransferase activity is lost in *A. fumigatus*.

Discussion

As important regulators of Ras protein localization and function, prenyltransferases have long been a focus for the development of novel anti-cancer therapeutics.²⁴⁻²⁶ Despite a conserved function among eukaryotes, recent evidence suggests that fungal farnesyltransferase enzymes could potentially serve as selective antifungal targets. Biochemical analyses have revealed key

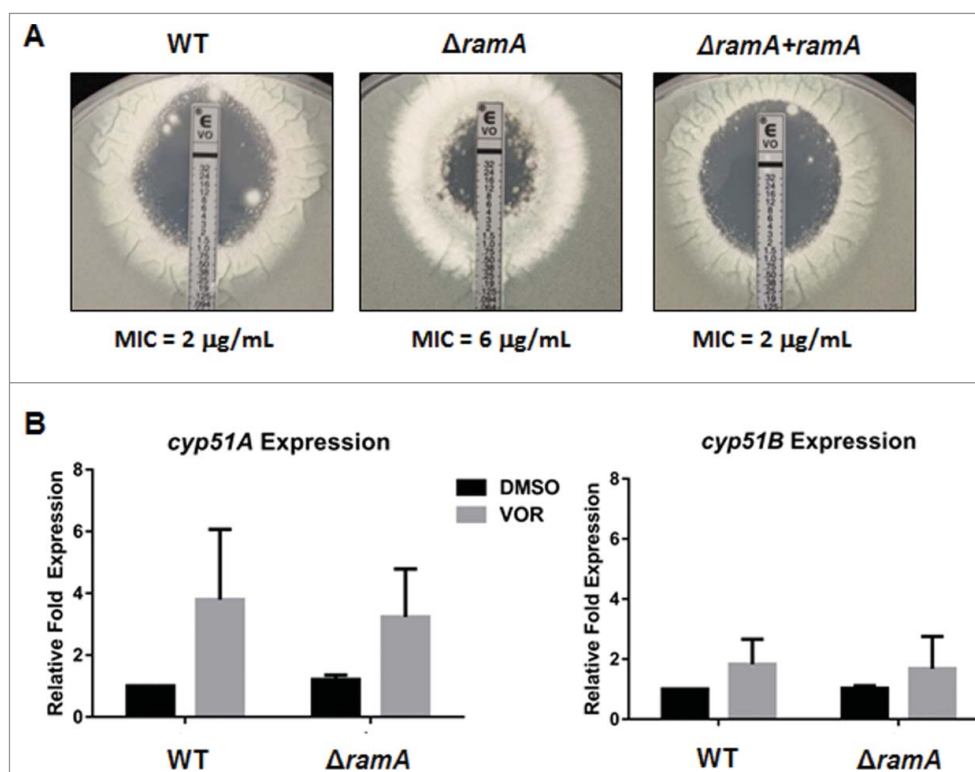


Figure 9. The $\Delta ramA$ mutant exhibits *cyp51A/B*-independent triazole resistance. (A) Antifungal susceptibility was performed by the E-test method, using a modified version of existing protocols. A conidial suspension of 1×10^6 conidia in 1 mL sterile water was spread on GMM+YE agar plates followed by application of E-test strips containing a voriconazole (VOR) concentration gradient of 0.002–32 $\mu\text{g/ml}$. Plates were incubated at 37°C and MIC values read at 48 h. (B) qRT-PCR analysis of *cyp51A* and *cyp51B* expression in the wild type (WT) and $\Delta ramA$ strains with and without voriconazole (VOR) treatment. WT and $\Delta ramA$ strains were grown in GMM+YE broth at 37°C with shaking at 250 rpm for 12 hours to generate young germlings. 50% MIC VOR (as determined by E-test shown in (A)) or equal volume of DMSO (vehicle control) was added and incubation continued for an additional 6 hours. qPCR was performed on total RNA using *A. fumigatus* tubulin (*tubA*) as the endogenous standard. Each sample was analyzed in technical triplicate, and the entire assay was performed 3 times. Measurements represent the mean of 3 independent experiments (\pm SD). Statistics were computed by 2-way ANOVA with Tukey's test for multiple comparisons (*, $p < 0.05$).

variations in the tertiary structure of the active site and product exit groove between *A. fumigatus* farnesyltransferase and the human homolog.^{27,28} These findings suggest that currently available farnesyltransferase inhibitors could be enhanced for selective toxic properties against fungal pathogens and re-purposed as anti-fungal agents.

Although data from the study of *Cryptococcus neoformans* suggest that deficiency of farnesyltransferase activity leads to reduced viability,^{10,29} no current reports of the importance of prenylation mechanisms in monomorphic molds exist. Our study with the *A. fumigatus* farnesyltransferase β -subunit, *ramA*, demonstrates that farnesylation influences multiple processes related to growth and development, likely through both RasA-dependent and RasA-independent mechanisms. For example, reduction of radial outgrowth and polarity establishment rates, aberrant nuclear positioning within hyphal compartments, hypersensitivity to chitin synthesis inhibition, and reduction in virulence are all phenotypes that were seen in the $\Delta ramA$ mutant but are also

induced by deletion or mislocalization of RasA.^{30,31} Therefore, RasA potentially mediates at least some aspect of these outcomes in the $\Delta ramA$ mutant. However, the altered partitioning of nuclei into conidia, the loss of hyphal polarity *in vivo* and the increased resistance to triazoles reported here for $\Delta ramA$ are not seen in *rasA* mutant strains³⁰⁻³³ (Fig. S1 and Table S2). As the protein substrates of prenylation pathways in fungi are expected to be expansive, it is assumed that these phenotypes are driven by mislocalization of additional farnesylated proteins.

The growth abnormalities reported here for the $\Delta ramA$ mutant, which displays RasA protein mislocalization, did not recapitulate the previously reported severe growth and morphological defects observed in other mutants with mislocalized RasA.^{15,31} The $\Delta ramA$ strain exhibited grossly normal hyphal morphology *in vitro*, a stark contrast to the stunted, hyper-branched hyphae of the RasA palmitoylation mutant (RasA^{C206/207S}), in which all RasA palmitoylation is abrogated and RasA is mislocalized to the cytosol and endo-

membranes.³¹ Although RasA localization was largely cytosolic upon loss of farnesyltransferase activity, a strong GFP signal was notably still present at septa, and small amounts of GFP-RasA were still visible at the plasma membrane. Together, these data suggest that the partial localization of RasA to membranes likely accounts for the lack of severe morphological defects in the $\Delta ramA$ mutant. However, RasA is entirely cytosolic with no septal localization in a prenylation-deficient RasA^{C210S} mutant,¹⁵ suggesting that the process of septal membrane targeting in the $\Delta ramA$ mutant is still prenylation-dependent. This finding indicates that RasA cross-prenylation, presumably by the geranylgeranyltransferase type-1 complex, occurs when the CAAX motif cysteine is intact. Cross-prenylation of proteins by both arms of the prenyltransferase pathway has been reported in other fungi, indicating that overlap of substrate specificity is a common phenomenon for these enzymes.^{34,35} Regardless, the possibility exists that the differential farnesylation or geranylgeranylation of RasA may have biologic significance. Distinct lipid anchors may function to target localization of the RasA protein to different membrane compartments for specific signaling outputs. This hypothesis, and whether it holds true for other *A. fumigatus* proteins, is under further study. To begin to delineate the potential for cross-prenylation in *A. fumigatus*, we have performed *in silico* analyses using the Prenylation Prediction Suite (PrePS) to identify potential CAAX-motif proteins and to predict their putative prenylation status.³⁶ Of 130 putative and verified genes encoding proteins with a carboxy-terminus that contain a cysteine at amino acid position -4 relative to the stop codon, only 28 are predicted to be prenylated CAAX-motifs (Table S3). The vast majority of these proteins are predicted to be modified by both farnesyl and geranylgeranyl moieties, suggesting promiscuous cross-prenylation for most CAAX-motif proteins in *A. fumigatus* (Table S3). In-depth biochemical analyses are required to assign substrate specificities for each prenyltransferase complex and to decipher whether additional CAAX motifs may serve as prenylation targets in *Aspergillus*.

Our virulence study is the first exploration of the importance of farnesyltransferase activity to the invasive growth of a monomorphic mold. While *ramA* deletion did not result in avirulence, as it does in the pathogenic yeast *C. neoformans*,¹⁰ virulence was attenuated, and the median onset of death was delayed. Statistical analysis of the $\Delta ramA$ and $2x\Delta ramA$ arms indicated no significant differences in survival between these 2 groups. These results suggest that the reduced virulence of the $\Delta ramA$ mutant is not simply due to the decreased conidial viability noted in our study, nor can it be solely attributed to

slow growth. Rather, it is likely that the host environment provides a further stress that negatively impacts virulence upon loss of *ramA*. In support of this hypothesis, the dysmorphic hyphal structures visible in lesions of the $\Delta ramA$ mutant, a phenotype not observed during standard *in vitro* culture, indicate that host-associated factors may exacerbate the growth deficiencies related to *ramA* deletion. We were only able to recapitulate swollen hyphal structures *in vitro* by treatment with the chitin synthesis inhibitor, nikkomycin Z. The $\Delta ramA$ mutant formed swollen hyphal segments at concentrations of nikkomycin Z that did not affect wild type growth. However, we noted no hypersensitivity of $\Delta ramA$ to the β -glucan synthesis inhibitor, caspofungin, indicating that the $\Delta ramA$ mutant is specifically defective at activating stress responses requiring regulation of chitin biosynthesis. Interestingly, our list of potentially prenylated proteins includes 2 uncharacterized homologs of a *S. cerevisiae* and *C. albicans* chitin-synthase regulator, *CHS4*, providing a mechanistic link to how the loss of farnesyltransferase activity may indirectly affect chitin synthase activity (Table S3). Deletion of *CHS4* in *S. cerevisiae* causes reduced chitin deposition and altered response to cell wall active compounds.³⁷ Therefore, it is conceivable that partial mislocalization of these putative chitin synthase regulators in *A. fumigatus*, via loss of prenylation, may alter the ability to activate chitin synthase enzymes in response to stress which, in turn, leads to the swollen hyphal phenotype *in vivo*. This interpretation implies that the lung environment is perceived as a cell wall stress by $\Delta ramA$. However, chitin synthase mutants have normal virulence levels in *A. fumigatus*, suggesting *in vivo* growth may not rely heavily on upregulation of the chitin biosynthesis machinery. Deletion of all 4 Family 2 chitin synthases in *A. fumigatus* leads to hyphal swelling similar to that seen with nikkomycin Z treatment and reminiscent of the *in vivo* growth defects of $\Delta ramA$.³⁸ In contrast to $\Delta ramA$, this phenotype is seen *in vitro* without additional exogenous stress and during *in vivo* invasive growth, and is not associated with reduced virulence.³⁸ Nevertheless, chitin biosynthesis in *A. fumigatus* is essential and requires the coordination of 8 chitin synthases that share overlapping functions. Therefore, the possibility exists that cell wall stress perceived by $\Delta ramA$ during *in vivo* growth results in the loss-of-polarity phenotype observed in the murine model of invasive aspergillosis. The contributions of farnesylation to cell wall stress response in *A. fumigatus* and the extent to which this stress response supports *in vivo* hyphal growth are under further study.

Because farnesyl pyrophosphate is a substrate for ergosterol biosynthesis, we also hypothesized that a mutation potentially altering utilization of the cellular

pool of farnesyl pyrophosphate, such as $\Delta ramA$, may affect the expression of downstream ergosterol biosynthesis genes and, therefore, sensitivity to antifungal drugs. The azole class of antifungal drugs binds and inactivates the rate-limiting enzymes in the ergosterol synthesis pathway, Cyp51A and Cyp51B,^{39–41} and overexpression of these target genes is a major mechanism of antifungal drug resistance.²² Although our data show that *ramA* deletion does alter triazole sensitivity, it does so in a manner that is not dependent on overexpression of *cyp51A* or *cyp51B*. These results suggest that farnesylation of a substrate protein may be required for its role in mediating susceptibility to inhibition of ergosterol biosynthesis. Further study of RamA-mediated resistance may be of value in augmenting our understanding of mechanisms behind triazole susceptibility in *A. fumigatus*.

In summary, we have established that the RamA farnesyltransferase β -subunit mediates diverse biologic processes critical to growth, development, and pathogenicity in *A. fumigatus*. These results accentuate the value of continuing to investigate prenylation pathways as regulators of multiple developmental processes in filamentous fungi and as therapeutic targets in the treatment of invasive fungal disease.

Materials and methods

A. *fumigatus* strains and growth conditions

A. fumigatus strain Af293 was used as the background strain for all mutants developed in this study. The $\Delta rasA$ and GFP-RasA strains used for antifungal susceptibility and RasA localization analyses, respectively, were previously developed.^{30,31} All strains were maintained on glucose minimal medium (GMM), as described previously,⁴² and conidia used for analyses were harvested from mycelia grown on GMM for 3 d at 37°C. GMM broth was used for assays requiring growth in submerged culture. Where indicated, GMM solid agar or broth were supplemented with 0.5% yeast extract (GMM+YE) to encourage robust growth. YPD (10% Yeast Extract, 20% Peptone, 20% Glucose) and RPMI-1640 (pH 7.0, buffered with MOPS) agar were also used for the examination of growth rate and conidiation. RPMI-1640 agar was used for triazole sensitivity assays by the E-test method.⁴³

Assays to mimic *in vivo* stress were performed as follows. Ten thousand conidia from each strain of the $\Delta ramA$ isogenic set were inoculated into 96-well plates containing GMM with serial dilutions of the following compounds: $CoCl_2$ (0.012–1.2 mM), Brefeldin A (0.1–100 $\mu g/ml$), dithiothreitol (0.01–10 mM), H_2O_2

(0.01–10 mM), or nikkomycin Z (0.1–100 $\mu g/ml$). For iron limitation stress, 10 thousand conidia from each strain were cultured in iron-free GMM broth or iron-free GMM broth plus 100 μM bathophenanthrolinedisulfonic acid. All cultures were incubated at 37°C for 24 hrs. After incubation, plates were examined and images were captured on a Nikon TS100 inverted microscope equipped with a DS-FI2 digital camera.

Construction of mutant strains

For the $\Delta ramA$ mutant, the entire *ramA* coding sequence was replaced with the hygromycin resistance cassette, as described previously.⁴⁴ Oligonucleotides used for genetic manipulations are listed in Table S1. Primer pairs P1/P2 and P3/P4 were used to amplify 1.5-kb regions upstream and downstream of the predicted *ramA* translational start site, respectively. The PCR-amplified upstream and downstream genomic DNA fragments were subcloned into pHygR³⁰ using *NotI* and *XhoI/KpnI* restriction sites, respectively, that were incorporated during amplification. The resulting vector was designated p $\Delta ramA$ -HygR. The full *ramA* deletion cassette was then PCR-amplified from vector p $\Delta ramA$ -HygR using primers P1/P4 and transformed into *A. fumigatus* protoplasts, using standard transformation protocols. Individual hygromycin-resistant colonies were isolated to GMM plates after 3 d of growth under hygromycin selection at 37°C. Transformants were initially screened for deletion of *ramA* by PCR using primers P5/P6, and then confirmed by Southern blot analysis.

Complementation of $\Delta ramA$ was achieved by ectopic integration of the *ramA* gene under the expression of the endogenous promoter. Primer pair P7/P8 was used to amplify a 3.2-kb fragment consisting of the *ramA* gene plus 1-kb of upstream native promoter sequence and 0.3-kb of downstream terminator sequence from the Af293 genome. The amplified fragment was subcloned as a *NotI/XbaI* insertion into vector pPhleoR. Vector pPhleoR was previously constructed by PCR-amplifying a phleomycin resistance cassette from vector pAN8–1 (Fungal Genetics Stock Center) using primer pair P9/P10 and sub-cloning this fragment into pBlueScript at the *HindIII* restriction site. The resulting transformation vector was linearized at a unique *XmnI* site in the backbone and transformed into $\Delta ramA$ protoplasts, which were plated under phleomycin selection (125 $\mu g/ml$) and incubated at 30°C. Phleomycin-resistant colonies were isolated to GMM plates. Primer pair P2/P11 was initially used to screen for $\Delta ramA$ complementation by PCR and subsequently confirmed by Southern blot analysis. Three reconstituted strains were produced, each with multiple integrations of the complementation

cassette. A strain with only 2 integrations was selected as the $\Delta ramA+ramA$ reconstituted strain for all subsequent experimentation. All noted phenotypes were complemented in the reconstituted strain.

For the analysis of RasA localization in the $\Delta ramA$ mutant, the described previously GFP-RasA expression vector,³¹ which expresses GFP-tagged RasA under the RasA native promoter, was used to transform the recipient $\Delta ramA$ strain. Transformants were screened for single-copy, ectopic integration and GFP fluorescence was analyzed using a Nikon NiU fluorescence microscope, equipped with a GFP filter.

Staining of the cell wall and nuclei

Existing protocols were slightly modified for nuclear and cell wall staining.^{14,30} Briefly, 1×10^5 conidia were incubated over sterile coverslips in GMM broth at 37°C for the indicated durations. Coverslips were washed twice for 10 min in 50 mM morpholinepropanesulfonic acid (MOPS) buffer (pH 6.7) and fixed in fixative solution (8% formaldehyde in 50 mM MOPS, 25 mM EGTA [pH 7.0], 5 mM MgSO₄, 5% DMSO, and 0.2% Triton-X) for 1 hr. Following fixation, coverslips were washed twice for 10 mins in MOPS buffer and incubated with 60 μ g/ml RNase A (ThermoScientific) for 1 hr at 37°C. Coverslips were then washed twice for 10 mins in MOPS buffer and inverted for 5 min onto a 0.5 ml drop of staining solution containing 12.5 μ g/ml propidium iodide (Sigma) and 1 μ g/ml Fluorescent Brightener 28 (Sigma). Finally, coverslips were washed twice for 10 mins in MOPS buffer and mounted for microscopy. Fluorescence microscopy was performed on a Nikon NiU microscope equipped with a Nikon DS-Qi1Mc camera using DAPI (4',6'-diamidino-2-phenylindole) and mCherry filter settings. Images were captured using Nikon Elements software (v4.0).

Ras activation assay

The Ras activation assay was performed as described previously.⁴⁵ Briefly, mature mycelia from the *ramA* isogenic set were harvested from cultures grown in GMM+YE broth at 37°C, 250 rpm, homogenized under liquid nitrogen, and resuspended in a 1:1 v/v ratio of lysis buffer containing Mg²⁺ and protease inhibitors (25 mM Tris-HCl [pH 7.5], 20 mM MgCl₂, 75 mM NaCl, 1 mM EDTA, 1% Igepal CA-630, 2% glycerol, 1:100 Pefabloc, 1:100 protein inhibitor cocktail [Sigma]). Lysates were centrifuged at 3500 rpm, 4°C, for 8 m, and supernatants were analyzed for total protein concentration via Bradford assay. GTP-bound RasA pull-down was then achieved using a Ras Activation Assay Kit (EMD Millipore #17-218), following

the manufacturer protocol. For each sample, 5 mg of total protein was incubated with Raf1-RBD coated beads for 45 mins at 4°C. Beads were pelleted by centrifugation at 13,000 rpm for 10 s, washed 3 times in 0.5 mL lysis buffer, and resuspended in 50 μ L lysis buffer. Washed beads were boiled to release bound protein and immediately loaded onto a 12% SDS-polyacrylamide gel (Bio-Rad). Control samples, for the detection of total RasA levels, consisted of 50 μ g crude lysate and were similarly boiled before SDS-PAGE separation. Membranes were probed with the anti-Ras, clone RAS10 mouse monoclonal primary antibody (1:2000 dilution, EMD Millipore) and followed by the secondary antibody, a horseradish peroxidase (HRP)-conjugated goat anti-mouse IgG2a (1:2000 dilution, Abcam). Blots were imaged using the Bio-Rad ChemiDoc XRS HQ System and QuantityOne software (v4.6.5, Bio-Rad). The ratio of GTP-bound RasA to total RasA in each strain was determined by densitometric analysis using ImageJ software. The assay was performed in biologic triplicate.

Analysis of *cyp51A* and *cyp51B* expression

A modification of a previously-described protocol for voriconazole treatment was used to generate mycelia for qRT-PCR analysis.²³ Briefly, 3×10^7 conidia of the wild type strain and 6×10^7 conidia of the $\Delta ramA$ strain were inoculated into GMM+YE broth and incubated at 37°C. After 12 hr incubation, a concentration of voriconazole solubilized in DMSO equal to 50% of the MIC for each strain as determined by E-test assay (Af293 = 1 μ g/ml; $\Delta ramA$ = 3 μ g/ml) was added to the treatment cultures. An equal volume of DMSO vehicle was added to control cultures of each strain. Incubation was continued at 37°C for 6 hr. Extraction of total RNA and synthesis of cDNA was performed using the Qiagen RNEasy Mini Kit and New England Biolabs ProtoScript II cDNA Synthesis Kit, respectively.

Biological triplicates of each treatment condition were analyzed by quantitative real-time PCR (qRT-PCR) in technical triplicate using *A. fumigatus tubA* (tubulin) as the endogenous standard. Target amplification primers for *cyp51A* (P12/ P13) and *cyp51B* (P14/P15) were as described previously.³⁹ The qRT-PCR analyses were conducted on an Applied Biosystems StepOne Real-Time PCR system, and data were analyzed by relative quantitation to wild type DMSO transcription levels using the $\Delta\Delta C_T$ method (StepOne Software, v2.2.2).

Virulence studies

All work was conducted with the formal approval of the University of South Alabama Institutional Animal Care

and Use Committee. A neutropenic murine model of IA was used to assess the effects of *ramA* deletion on survival and disease pathology. Six-week-old male CF-1 mice (Charles River) were immunosuppressed according to a previously-described neutropenic model.¹⁶ In brief, immunosuppression was achieved with cyclophosphamide (150 mg/kg of body weight) injected intraperitoneally at 3 d before conidial inoculation, and 3 and 7 d post-inoculation; and triamcinolone acetonide (40 mg/kg of body weight) injected subcutaneously at 1 day before inoculation. Freshly-harvested conidia of the wild type and $\Delta ramA$ strains were inoculated intranasally at a dose of 1×10^5 conidia in a 20 μ l volume of sterile, pyrogen-free cell culture water (EMD Millipore) on Day 0 ($n = 14$ mice per strain treatment group). An additional treatment group was inoculated with a double concentration of $\Delta ramA$ conidia (2×10^5 conidia) to account for the observed conidial viability deficit in the $\Delta ramA$ strain. Mice were transiently anesthetized with 3.5% isoflurane before conidial inoculation. Mortality was monitored for the ensuing 14 days, and moribund mice killed by CO₂ euthanasia. Survival was plotted on a Kaplan-Meier curve. Pairwise survival comparisons of all treatment groups vs. the wild type strain were performed by Kruskal-Wallis (nonparametric one-way ANOVA) analysis with Dunn's post-hoc testing (GraphPad Prism v6).

Analysis of fungal burden and histopathology

For analysis of fungal burden, fresh lung tissue of the entire right lung was processed as described previously.¹⁷ Briefly, lungs from each treatment arm were homogenized and lysed in equal volumes of lysis buffer (1 M Tris-HCl, 250 mM EDTA [pH 8.0], 5 M NaCl, 10% SDS, 10 mg/ml Proteinase K) and 0.9% saline solution. Lysed lungs were incubated for 18 h at 56°C and the total genomic DNA was extracted as described previously.³³ Quantitative-PCR (qPCR) analysis was performed in technical triplicate for each sample using established amplification primers P16 and P17 (Table S1) to amplify a region of the *A. fumigatus* 18S rRNA gene.¹⁷ Each sample reaction was performed in PrimeTime® Gene Expression Master Mix (Integrated DNA Technologies). qPCR was conducted on a Bio-Rad CFX96 Real-Time PCR system running Bio-Rad CFX Manager software (v1.1). DNA amplification in infected samples was analyzed by normalization to mean transcription levels in uninfected control samples by the ΔC_T method. Statistical analysis to compare relative signals between each strain treatment was performed using one-way ANOVA with Dunnett's test for multiple comparisons.

For analysis of histopathology, 6-week-old male CF-1 mice (Charles River) were immunosuppressed,

inoculated with conidia, and killed according to the regimen described above ($n = 2$ mice per strain treatment group). Thoracotomy was performed, and lungs were inflated with approximately 1 mL of a 10% buffered formalin solution (10% v/v 37% formaldehyde, 4 g/L monobasic sodium phosphate, 6.5 g/L dibasic sodium phosphate) and removed from the carcass. The superior, middle, and inferior lobes of the right lung were each sectioned transversely into 3 slices and submitted in 10% buffered formalin to the University of South Alabama Medical Center Electron Microscopy Laboratory (Mobile, AL) for paraffin embedding. Paraffin-embedded blocks were then submitted to the University of Tennessee Health Science Center Dermatopathology Laboratory (Memphis, TN) for microtome sectioning and staining. Two serial 5- μ m sections were cut from the blocks; one section was stained with Gomori methenamine silver (GMS) stain and the other with hematoxylin and eosin (H&E). These stains were chosen to evaluate fungal growth and host inflammatory response in the neutropenic immunosuppression model. The presence of fungal hyphae and/or inflammatory nuclei was assessed by microscopy.

Disclosure of potential conflicts of interest

No potential conflicts of interest were disclosed.

Funding

This work was supported by NIH grant R01AI106925 to JRF.

References

- [1] Casey PJ, Seabra MC. Protein Prenyltransferases. *J Biol Chem* 1996; 271:5289-92; PMID:8621375; <https://doi.org/10.1074/jbc.271.10.5289>
- [2] Seabra MC, Reiss Y, Casey PJ, Brown MS, Goldstein JL. Protein farnesyltransferase and geranylgeranyltransferase share a common α subunit. *Cell* 1991; 65:429-34; PMID:2018975; [https://doi.org/10.1016/0092-8674\(91\)90460-G](https://doi.org/10.1016/0092-8674(91)90460-G)
- [3] Omer CA, Gibbs JB. Protein prenylation in eukaryotic microorganisms: genetics, biology and biochemistry. *Mol Microbiol* 1994; 11:219-25; PMID:8170384; <https://doi.org/10.1111/j.1365-2958.1994.tb00302.x>
- [4] Zhang FL, Casey PJ. Protein Prenylation: Molecular Mechanisms and Functional Consequences. *Ann Rev Biochem* 1996; 65:241-69; PMID:8811180; <https://doi.org/10.1146/annurev.biochem.65.1.241>
- [5] Scott Reid T, Terry KL, Casey PJ, Beese LS. Crystallographic Analysis of CaaX Prenyltransferases Complexed with Substrates Defines Rules of Protein Substrate Selectivity. *J Mol Biol* 2004; 343:417-33; PMID:15451670; <https://doi.org/10.1016/j.jmb.2004.08.056>

- [6] Moores SL, Schaber MD, Mosser SD, Rands E, O'Hara MB, Garsky VM, Marshall MS, Pompliano DL, Gibbs JB. Sequence dependence of protein isoprenylation. *J Biol Chem* 1991; 266:14603-10; PMID:1860864
- [7] Song JL, White TC. RAM2: an essential gene in the prenylation pathway of *Candida albicans*. *Microbiology* 2003; 149:249-59; PMID:12576598; <https://doi.org/10.1099/mic.0.25887-0>
- [8] He B, Chen P, Chen S-Y, Vancura KL, Michaelis S, Powers S. RAM2, an essential gene of yeast, and RAM1 encode the two polypeptide components of the farnesyltransferase that prenylates a-factor and Ras proteins. *PNAS* 1991; 88:11373-7; PMID:1763050; <https://doi.org/10.1073/pnas.88.24.11373>
- [9] Yang W, Urano J, Tamanoi F. Protein farnesylation is critical for maintaining normal cell morphology and canavanine resistance in *Schizosaccharomyces pombe*. *J Biol Chem* 2000; 275:429-38; PMID:10617635; <https://doi.org/10.1074/jbc.275.1.429>
- [10] Esher SK, Ost KS, Kozubowski L, Yang D-H, Kim MS, Bahn Y-S, Alspaugh JA, Nichols CB. Relative Contributions of Prenylation and Postprenylation Processing in *Cryptococcus neoformans* Pathogenesis. *mSphere* 2016; 1(2):e00084-15; PMID:27303728
- [11] Lin S-J, Schranz J, Teutsch SM. Aspergillosis Case-Fatality Rate: Systematic Review of the Literature. *Clin Infect Dis* 2001; 32:358-66; PMID:11170942
- [12] Al Abdallah Q, Fortwendel JR. Exploration of *Aspergillus fumigatus* Ras pathways for novel antifungal drug targets. *Front Microbiol* 2015; 6:128; PMID:25767465.
- [13] Ishi K, Maruyama JI, Juvvadi PR, Nakajima H, Kitamoto K. Visualizing Nuclear Migration during Conidiophore Development in *Aspergillus nidulans* and *Aspergillus oryzae*: Multinucleation of Conidia Occurs through Direct Migration of Plural Nuclei from Phialides and Confers Greater Viability and Early Germination in *Aspergillus oryzae*. *Biosci Biotech Biochem* 2005; 69:747-54.
- [14] Momany M, Taylor I. Landmarks in the early duplication cycles of *Aspergillus fumigatus* and *Aspergillus nidulans*: polarity, germ tube emergence and septation. *Microbiology* 2000; 146:3279-84; PMID:11101686
- [15] Norton TS, Fortwendel JR. Control of Ras-Mediated Signaling in *Aspergillus fumigatus*. *Mycopathologia* 2014; 178(5-6):325-30:1-6.
- [16] Fortwendel JR, Zhao W, Bhabhra R, Park S, Perlin DS, Askew DS, Rhodes JC. A Fungus-Specific Ras homolog contributes to the Hyphal growth and virulence of *Aspergillus fumigatus*. *Eukaryot Cell* 2005; 4:1982-9; PMID:16339716
- [17] Bowman JC, Abruzzo GK, Anderson JW, Flattery AM, Gill CJ, Pikounis VB, Schmatz DM, Liberator PA, Douglas CM. Quantitative PCR assay to measure *Aspergillus fumigatus* burden in a Murine model of Disseminated Aspergillosis: Demonstration of efficacy of Caspofungin Acetate. *Antimicrob Agents Chemother* 2001; 45:3474-81; PMID:11709327
- [18] Richie DL, Hartl L, Amanianda V, Winters MS, Fuller KK, Miley MD, White S, McCarthy JW, Latgé JP, Feldmesser M, et al. A Role for the Unfolded Protein Response (UPR) in Virulence and Antifungal Susceptibility in *Aspergillus fumigatus*. *PLoS Pathog* 2009; 5:e1000258; PMID:19132084
- [19] Schrettl M, Beckmann N, Varga J, Heinekamp T, Jacobsen ID, Jöchl C, Moussa TA, Wang S, Gsaller F, Blatzer M, et al. HapX-mediated adaptation to iron starvation is crucial for virulence of *Aspergillus fumigatus*. *PLOS Pathog* 2010; 6:e1001124; PMID:20941352; <https://doi.org/10.1371/journal.ppat.1001124>
- [20] Lee H, Bien CM, Hughes AL, Espenshade PJ, Kwon-Chung KJ, Chang YC. Cobalt chloride, a hypoxia-mimicking agent, targets sterol synthesis in the pathogenic fungus *Cryptococcus neoformans*. *Mol Microbiol* 2007; 65:1018-33; PMID:17645443; <https://doi.org/10.1111/j.1365-2958.2007.05844.x>
- [21] Guinea J, Peláez T, Alcalá L, Bouza E. Correlation between the E test and the CLSI M-38 A microdilution method to determine the activity of amphotericin B, voriconazole, and itraconazole against clinical isolates of *Aspergillus fumigatus*. *Diagnost Microbiol Infect Dis* 2007; 57:273-6; <https://doi.org/10.1016/j.diagmicrobio.2006.09.003>
- [22] Gonçalves SS, Souza ACR, Chowdhary A, Meis JF, Colombo AL. Epidemiology and molecular mechanisms of antifungal resistance in *Candida* and *Aspergillus*. *Mycoses* 2016; 59:198-219; <https://doi.org/10.1111/myc.12469>
- [23] Blosser SJ, Cramer RA. SREBP-Dependent Triazole Susceptibility in *Aspergillus fumigatus* is mediated through Direct Transcriptional Regulation of *erg11A* (*cyp51A*). *Antimicrob Agents Chemother* 2012; 56:248-57; PMID:22006005; <https://doi.org/10.1128/AAC.05027-11>
- [24] Sepp-Lorenzino L, Ma Z, Rands E, Kohl NE, Gibbs JB, Oliff A, Rosen N. A Peptidomimetic inhibitor of Farnesyl: Protein transferase blocks the anchorage-dependent and -independent growth of human tumor cell lines. *Can Res* 1995; 55:5302-9.
- [25] Appels NMGM, Beijnen JH, Schellens JHM. Development of Farnesyl Transferase Inhibitors: A Review. *Oncologist* 2005; 10:565-78; PMID:16177281; <https://doi.org/10.1634/theoncologist.10-8-565>
- [26] Philips MR, Cox AD. Geranylgeranyltransferase I as a target for anti-cancer drugs. *J Clin Invest* 2007; 117:1223-5; PMID:17476354; <https://doi.org/10.1172/JCI32108>
- [27] Hast MA, Nichols CB, Armstrong SM, Kelly SM, Hellinga HW, Alspaugh JA, Beese LS. Structures of *Cryptococcus neoformans* Protein Farnesyltransferase Reveal Strategies for Developing Inhibitors That Target Fungal Pathogens. *J Biol Chem* 2011; 286:35149-62; PMID:21816822; <https://doi.org/10.1074/jbc.M111.250506>
- [28] Mabanglo MF, Hast MA, Lubock NB, Hellinga HW, Beese LS. Crystal structures of the fungal pathogen *Aspergillus fumigatus* protein farnesyltransferase complexed with substrates and inhibitors reveal features for antifungal drug design. *Prot Sci* 2014; 23:289-301; <https://doi.org/10.1002/pro.2411>
- [29] Vallim MA, Fernandes L, Alspaugh JA. The RAM1 gene encoding a protein-farnesyltransferase {beta}-subunit homologue is essential in *Cryptococcus neoformans*. *Microbiology* 2004; 150:1925-35; PMID:15184578; <https://doi.org/10.1099/mic.0.27030-0>
- [30] Fortwendel JR, Fuller KK, Stephens TJ, Bacon WC, Askew DS, Rhodes JC. *Aspergillus fumigatus* RasA regulates asexual development and cell wall integrity.

- Eukaryot Cell 2008; 7:1530-9; PMID:18606827; <https://doi.org/10.1128/EC.00080-08>
- [31] Fortwendel JR, Juvvadi PR, Rogg LE, Asfaw YG, Burns KA, Randell SH, Steinbach WJ. Plasma membrane localization is required for RasA-mediated polarized morphogenesis and virulence of *Aspergillus fumigatus*. Eukaryot Cell 2012; 11:966-77; PMID:22562470; <https://doi.org/10.1128/EC.00091-12>
- [32] Fortwendel JR, Juvvadi PR, Rogg LE, Steinbach WJ. Regulatable Ras Activity is critical for Proper Establishment and Maintenance of Polarity in *Aspergillus fumigatus*. Eukaryot Cell 2011; 10:611-5; PMID:21278230; <https://doi.org/10.1128/EC.00315-10>
- [33] Fortwendel JR, Panepinto JC, Seitz AE, Askew DS, Rhodes JC. *Aspergillus fumigatus* *rasA* and *rasB* regulate the timing and morphology of asexual development. Fung Genet Biol 2004; 41:129-39; <https://doi.org/10.1016/j.fgb.2003.10.004>
- [34] Trueblood CE, Ohya Y, Rine J. Genetic evidence for in vivo cross-specificity of the CaaX-box protein prenyltransferases farnesyltransferase and geranylgeranyltransferase-I in *Saccharomyces cerevisiae*. Mol Cell Biol 1993; 13:4260-75; PMID:8321228; <https://doi.org/10.1128/MCB.13.7.4260>
- [35] Kelly R, Card D, Register E, Mazur P, Kelly T, Tanaka K-I, Onishi J, Williamson JM, Fan H, Satoh T, et al. Geranylgeranyltransferase I of *Candida albicans*: Null mutants or enzyme inhibitors produce unexpected Phenotypes. J Bacteriol 2000; 182:704-13; PMID:10633104; <https://doi.org/10.1128/JB.182.3.704-713.2000>
- [36] Maurer-Stroh S, Koranda M, Benetka W, Schneider G, Sirota FL, Eisenhaber F. Towards Complete Sets of Farnesylated and Geranylgeranylated Proteins. PLOS Comp Biol 2007; 3:e66; <https://doi.org/10.1371/journal.pcbi.0030066>
- [37] Trilla JA, Cos T, Duran A, Roncero C. Characterization of CHS4 (CAL2), a Gene of *Saccharomyces cerevisiae* Involved in Chitin Biosynthesis and Allelic to SKT5 and CSD4. Yeast 1997; 13:795-807; PMID:9234668; [https://doi.org/10.1002/\(SICI\)1097-0061\(199707\)13:9%3c795::AID-YEA139%3e3.3.CO;2-C10.1002/\(SICI\)1097-0061\(199707\)13:9%3c795::AID-YEA139%3e3.0.CO;2-L](https://doi.org/10.1002/(SICI)1097-0061(199707)13:9%3c795::AID-YEA139%3e3.3.CO;2-C10.1002/(SICI)1097-0061(199707)13:9%3c795::AID-YEA139%3e3.0.CO;2-L)
- [38] Muszkieta L, Aimanianda V, Mellado E, Gribaldo S, Alcázar-Fuoli L, Szweczyk E, Prevost MC, Latgé JP. Deciphering the role of the chitin synthase families 1 and 2 in the *in vivo* and *in vitro* growth of *Aspergillus fumigatus* by multiple gene targeting deletion. Cell Microbiol 2014; 16:1784-805; PMID:24946720; <https://doi.org/10.1111/cmi.12326>
- [39] Mellado E, Diaz-Guerra TM, Cuenca-Estrella M, Rodriguez-Tudela JL. Identification of two different 14- α Sterol Demethylase-Related Genes (*cyp51A* and *cyp51B*) in *Aspergillus fumigatus* and Other *Aspergillus* species. J Clin Microbiol 2001; 39:2431-8; PMID:11427550; <https://doi.org/10.1128/JCM.39.7.2431-2438.2001>
- [40] Alcazar-Fuoli L, Mellado E, Garcia-Effron G, Lopez JF, Grimalt JO, Cuenca-Estrella JM, Rodriguez-Tudela JL. Ergosterol biosynthesis pathway in *Aspergillus fumigatus*. Steroids 2008; 73:339-47; PMID:18191972; <https://doi.org/10.1016/j.steroids.2007.11.005>
- [41] Bossche HV, Koymans L, Moereels H. P450 inhibitors of use in medical treatment: Focus on mechanisms of action. Pharmacol Therapeut 1995; 67:79-100; [https://doi.org/10.1016/0163-7258\(95\)00011-5](https://doi.org/10.1016/0163-7258(95)00011-5)
- [42] Fortwendel JR, Juvvadi PR, Pinchai N, Perfect BZ, Alspaugh JA, Perfect JR, Steinbach WJ. Differential Effects of Inhibiting Chitin and 1,3- β -D-Glucan Synthesis in Ras and Calcineurin Mutants of *Aspergillus fumigatus*. Antimicrob Agents Chemother 2009; 53:476-82; PMID:19015336; <https://doi.org/10.1128/AAC.01154-08>
- [43] Espinel-Ingroff A, Rezusta A. E-Test Method for Testing Susceptibilities of *Aspergillus* spp. to the New Triazoles Voriconazole and Posaconazole and to Established Antifungal Agents: Comparison with NCCLS Broth Microdilution method. J Clin Microbiol 2002; 40:2101-7; PMID:12037072; <https://doi.org/10.1128/JCM.40.6.2101-2107.2002>
- [44] Yelton MM, Hamer JE, Timberlake WE. Transformation of *Aspergillus nidulans* by using a *trpC* plasmid. PNAS 1984; 81:1470-4; PMID:6324193; <https://doi.org/10.1073/pnas.81.5.1470>
- [45] Al Abdallah Q, Norton TS, Hill AM, LeClaire LL, Fortwendel JR. A Fungus-Specific Protein Domain is essential for RasA-Mediated Morphogenetic signaling in *Aspergillus fumigatus*. mSphere 2016; 1 (6): e00234-16; PMID:27921081; <https://doi.org/10.1128/mSphere.00234-16>